Ionogel-Templated Synthesis and Organization of Anisotropic Gold Nanoparticles

Millicent A. Firestone,* Mark L. Dietz, Sönke Seifert, Susana Trasobares, Dean J. Miller, and Nestor J. Zaluzec

Photochemical reduction of tetrachloroaurate ($AuCl_4^-$) ions in the highly constrained aqueous domains of a nanostructured ionogel template, formed via self-assembly of the ionic liquid 1-decyl-3-methyl-imidazolium chloride ($C_{10}mim^+Cl^-$) in water, results in the formation of anisotropic gold nanoparticles with a variety of sizes and morphologies, which include previously unattainable trigonal prismatic nanorods. Unexpectedly, small-angle X-ray scattering studies of the Au–ionogel composite reveal that the in situ formation of the nanoparticles increases the mesoscopic order of the ionogel, which results in its conversion to a near-monodomain structure. The findings demonstrate that nanostructured, ionic liquid-based gels can be used to template the formation of new nanoparticle morphologies with technologically important optical, electronic, and catalytic properties. It may also be possible to design soft templates that permit the fabrication of highly ordered nanoparticle array–hydrogel composites, thereby enabling control and tuning of the collective properties of the encapsulated nanoparticles.

Keywords:
· gels
· gold
· nanoparticles
· photoreduction
· template synthesis

1. Introduction

Recognition of the unique physicochemical properties and the potential technological utility of inorganic nanoparticles has led to considerable recent effort to develop facile methods for their synthesis and organization.[1] Studies of nanoparticulate noble metals are particularly important given their potential as catalysts,[2] optical filters,[3] plasmonic waveguides,[4,5] and bio- or chemosensors.[6,7] Although the behavior of nanoparticle-based systems is influenced by their chemical environment[8] and packing arrangement,[9] their intrinsic properties are determined first and foremost by their size and shape. Anisotropic metal nanoparticles exhibit optical properties of significant technological interest including enhanced fluorescence,[10] nonlinear optical properties, optical resonances in the near infrared (NIR), and orientation-dependent plasmon excitation,[11] all factors important in their potential application in, for example, optoelectronics. In addition, unlike spherical nanoparticles, anisotropic nanoparticles often possess different atomic planes and/or increased surface area that can be exploited for enhanced or selective catalysis of a variety of chemical reactions.[12] Finally, rod- or wire-shaped metal nanoparticles offer the possibility of serving as interconnects for the assembly and integration of molecular-scale components into electronic devices.[13,14] For these reasons, there has been increasing interest in the development of means to produce nonspherical nanoparticles.

[*] Dr. M. A. Firestone, Dr. S. Trasobares, Dr. D. J. Miller,
Dr. N. J. Zaluzec
Materials Science Division, Argonne National Laboratory
9700 South Cass Avenue, Argonne, IL 60439 (USA)
Fax: (+1) 630-252-9151
E-mail: firestone@anl.gov
Dr. M. L. Dietz
Chemistry Division, Argonne National Laboratory
9700 South Cass Avenue, Argonne, IL 60439 (USA)
Dr. S. Seifert
Advanced Photon Source Division, Argonne National Laboratory
9700 South Cass Avenue, Argonne, IL 60439 (USA)

Two general approaches to the synthesis of anisotropic nanoparticles, termed "hard-template" and "soft-template" methods, have been described. In the former, the metal of interest (e.g., gold) is electrodeposited in the pores of any of a variety of nanoporous membranes, such as anodized alumina,[15,16] etch-tracked polycarbonate,[17,18] or mesoporous silica.[19] Hard templates provide a rigid organizing matrix for in situ synthesis and, in principle, a means of controlling particle orientation, but their use typically requires tedious, multistep procedures that include fabrication of the ordered templates, electrodeposition of the nanoparticles, and lengthy and often difficult procedures for isolation of the formed nanoparticles from the template. The use of soft templates (e.g., organized media such as micelles, vesicles, liquid crystals, or microemulsions) offers an attractive alternative as a means to direct and control nanoparticle growth, which provides for the facile (i.e., one-step) synthesis of nanoparticles and their ready recovery.[20–23] In addition, soft templates exhibit a wide diversity of structural motifs, and thus can be exploited to provide particle morphologies other than the cylindrical, rod-shaped materials typically produced by porous membranes. Finally, soft materials can be processed to promote or tune domain alignment,[24] thus offering a way to control both the polydispersity and aspect ratio of asymmetric particles.[21] Unfortunately, soft templates typically do not offer the ability to simultaneously achieve in situ particle growth, anisotropic particle orientation, *and* controlled organization within the matrix, an important step in harnessing the unique properties of the nanoparticles for nanoscale devices.[25]

Recognition of the possibilities afforded by ionic liquids (ILs) as alternatives to conventional molecular solvents in the synthesis of organic compounds[26–28] has recently led to growing interest in their application in the preparation of novel materials.[28–33] A few reports have described the synthesis of metal nanoparticles in ILs,[34–38] but without exception the particles obtained have been spherical. Recently, however, Zhu et al.[39] reported that single-crystalline nanorods and nanowires of tellurium could be prepared in an ionic liquid by microwave irradiation of a solution of an appropriate precursor in the presence of a reductant. The production of nonspherical nanoparticles in this instance was attributed to the microwave-induced generation of transient, anisotropic nanodomains in the solvent, which facilitated the anisotropic growth of Te nanoparticles. These results suggest that wet ionic liquids, which as has been noted previously[29,40] are nanostructured anisotropic solvents, should represent a medium favorable to the production of nonspherical nanoparticles.

Herein, we demonstrate that the lyotropic, liquid-crystalline hydrogel formed upon addition of water to certain *N,N'*-dialkylimidazolium-based ionic liquids[29] constitutes a unique soft template capable of providing for the in situ growth of anisotropic gold nanoparticles of a variety of sizes and morphologies, which include previously unattainable trigonal prismatic nanorods. In addition, we show that the ionogel offers the potential to create a periodic array of the nanoparticles (i.e., to control particle aggregation and packing) within the template, an important property given that the utility of metal nanoparticles in nanoscale devices will ultimately depend not only on their synthesis, but also on control of their orientation and organization.

2. Results and Discussion

Prior work in this laboratory has demonstrated that addition of water to the ionic liquid 1-decyl-3-methylimidazolium bromide ($C_{10}mim^+Br^-$) can trigger its spontaneous conversion to a highly viscous, nanostructured, lamellar gel phase[29], termed an "ionogel".[32] This behavior is not confined to the bromide form of the ionic liquid; in fact, $C_{10}mim^+Cl^-$, an ionic liquid also comprising a hydrophilic anion and a 1-alkyl-3-methylimidazolium cation bearing a long alkyl chain, forms a similar gel-phase nanostructure upon addition of an appropriate concentration of water.[33] Both of these materials feature highly constrained water channels, which suggests their potential utility as templates for the formation of nanosize metal particles.
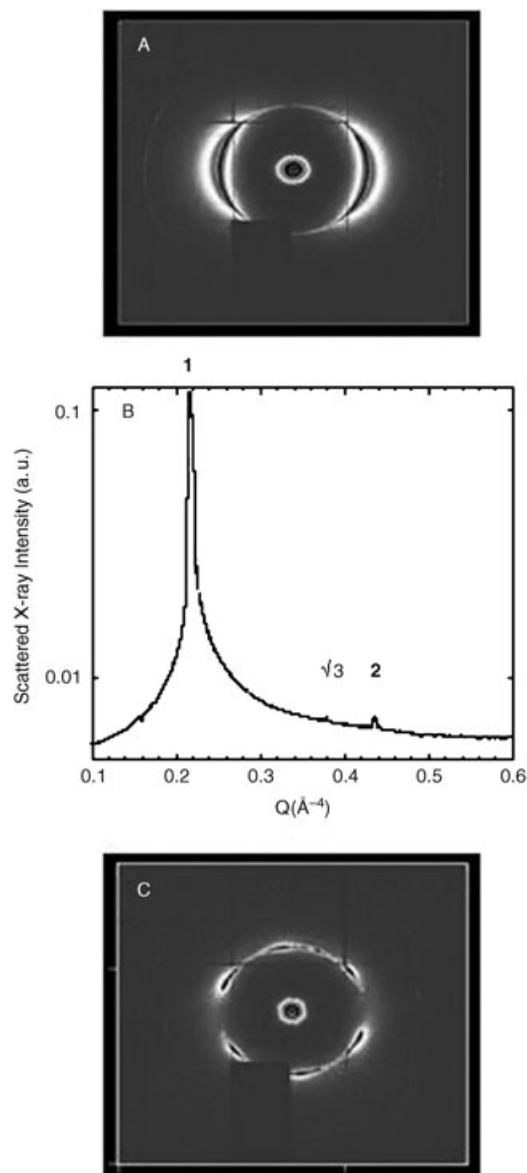
Brief irradiation of a tetrachloroaurate-laden $C_{10}mim^+Cl^-$ ionogel with ultraviolet light results in a color change from pale yellow to an iridescent pink, consistent with reduction of $AuCl_4^-$ to Au^0 (purplish-blue hues are also observed, depending on how the viewing light interacts with the sample).[41] The post-irradiation color of the Au–ionogel composite is readily evident in the optical micrograph presented in Figure 1 A. Polarized optical micrographs of a sample before and after irradiation are presented in Figure 1 B and C, respectively. As can be seen, even after UV irradiation, the liquid-crystalline textures associated with the original ionogel are retained. In fact, both samples display numerous focal conic textures suggestive of a columnar hexatic liquid-crystalline phase. Also noteworthy in the latter sample (Figure 1 C) is the presence of numerous black streaks not observed prior to UV irradiation that may, in fact, be regions of organized gold nanoparticles.

The mesoscopic structure of the Au–ionogel composite was determined by small-angle X-ray scattering (SAXS). When the incident X-ray beam is perpendicular to the long axis of the capillary, a 2D SAXS pattern in which the scattered X-ray intensity is predominantly directed equatorially is observed (Figure 2 A). The azimuthally averaged data (Figure 2 B) show the presence of three Bragg peaks at $1:\sqrt{3}:2$ ($q = 0.21$, 0.38, and 0.44 Å^{-1}), which indicates a 2D hexagonal lattice. The position of the first-order peak can be used to determine a lattice parameter, $a = (2/\sqrt{3})d_{100} = 34.0$ Å, based on the d_{100} spacings of 29.6 Å. A spot pattern displaying six intense (10) reflections with sixfold symmetry (Figure 2 C) is observed upon rotation of the sample. Such a pattern is characteristic of a 2D hexagonal lattice in which the hexagonal cylinders are arranged primarily coincident with the incident X-rays. These results differ from those observed for a randomly oriented liquid-crystalline material, which would exhibit a circular, isotropic 2D diffraction pattern. The relatively well-resolved Bragg diffraction spots indicate that the Au–ionogel composite consists primarily of large, hexagonal domains over the sample volume (ca. 50 μm^2) interrogated by the X-ray beam. Achieving such a
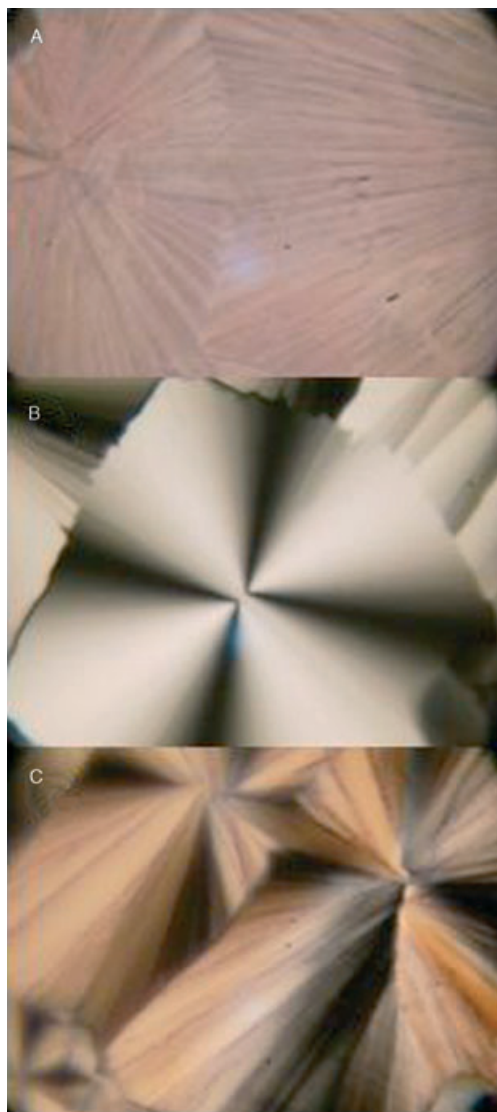
Figure 1. A) Optical micrograph of a thin film of $C_{10}mim^+Cl^-$ containing about 16% (w/w) of a 0.02 M aqueous solution of $HAuCl_4$ following 70 min irradiation with 254-nm light. B) Polarized optical micrograph of the same sample before UV irradiation. C) Polarized optical micrograph of the same thin film after 70 min irradiation with 254-nm light.


Figure 2. A) 2D small-angle X-ray scattering pattern for a $C_{10}mim^+Cl^-$ sample containing about 16% (w/w) 0.02 M aqueous $HAuCl_4$ after UV irradiation. The sample is confined in a 1.5-mm quartz capillary with the long axis perpendicular to the incident beam. B) Azimuthally averaged data from (A). C) SAXS of the same sample after rotation with respect to the incident X-ray beam.

high degree of alignment in a self-assembled material without the use of post-self-assembly processing is uncommon in liquid-crystalline systems.[42] Interestingly, this high degree of order is apparently induced by the in situ formation of the gold nanoparticles. That is, prior to the photochemical reduction of the added Au^{III}, the ionogel matrix exhibits a sheetlike structure similar to that reported previously[29] for $C_{10}mim^+Br^-$. The observed structural conversion may arise from the well-established epitaxial relationship between lamellar and hexagonal structures.[43,44] It has been proposed that in a long-lived nonequilibrium state, a hexagonal perforated layer (HPL)-type structure can form, which comprises a binary system where one of the components (presumably the water and associated anions in this system) penetrates layers of the second component (here, $C_{10}mim^+$) via hexag-

onally arranged channels that serve to connect the layers. These results suggest that the gold nanoparticles within the water domains of the hydrogel may interact synergistically (either electrostatically or topologically) with the matrix in such a way as to enhance long-range, mesoscopic order. Such an observation runs counter to the more common case, in which the introduction of a guest species typically causes a loss in spatial coherence of the host matrix.[45]

To gain insight into the morphology of the nanoparticles formed within the ionogel, UV/Vis–NIR studies of the composite were carried out (Figure 3 A). In contrast to the extinction spectrum (defined as the sum of the absorption and scattering spectra measured in transmission mode)[46] typi-
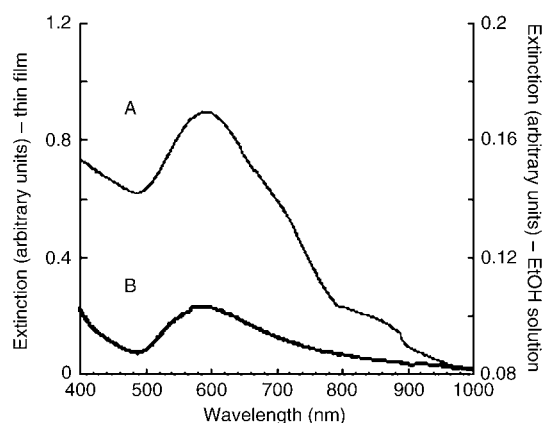
Figure 3. UV/Vis–NIR transmission optical spectrum collected on A) a thin, supported film of $C_{10}mim^+Cl^-$ containing about 16 % (w/w) 0.02 M aqueous $HAuCl_4$ after UV irradiation for 40 min and B) an ethanolic solution of the thin film in (A).

cally observed for spherical gold nanoparticles, which features a single surface plasmon resonance (SPR) at ≈ 525 nm[47,48], the UV/Vis–NIR spectrum of the composite exhibits a broad, prominent peak centered at about 590 nm which bears a shoulder at 660–760 nm, along with a second band at 796–896 nm. Prior work has shown that the position of the 525-nm resonance typically changes only slightly as the dielectric constant of the surrounding medium is changed[48] or surface adsorbates are added, in particular cationic surfactants such as cetyltrimethylammonium bromide (CTAB, whose structural similarity to certain ionic liquids has been noted previously[30]). Particle size and aggregation also have relatively little effect on the position of this resonance (but can give rise to bands in the NIR region).[48] Changes in particle shape, however, have been demonstrated both theoretically and experimentally to produce more pronounced shifts in the SPR of nanoparticles of coinage metals.[49] This finding suggests that the SPR observed at 590 nm in the Au–ionogel spectrum may signal the formation of nonspherical nanoparticles.[50]

The formation of tight aggregates by the assembly of smaller nanoparticles and electronic coupling/communication between nanoparticles imposed by their confinement[51] within the organized ionogel matrix represent possible explanations for the mid-wavelength (ca. 660–760 nm) absorbance feature. This band, as well as the longer wavelength absorbance band centered at about 850 nm, is also consistent with the formation of nonspherical particles. That is, it is well known that asymmetric nanoparticles can give rise to several SPR bands. Cylindrical rodlike particles, for example, exhibit two such bands, a transverse band located at ≈ 525 nm and a broadened, red-shifted longitudinal resonance, the exact position of which (between ca. 600 and 900 nm) depends on the length of the rod.[52,53] Tetrahedral gold nanocrystals exhibit a similar absorption spectrum comprising a pair of SPM bands.[54] Circular nanodisks (with $C_{\infty h}$ symmetry) and triangular nanoplates (with D_{3h} symmetry) are also expected to yield multiple (two or three, respectively) SPR peaks.[47] Thus, the appearance of three

bands in this system is consistent with either nanoparticle aggregation, the formation of several distinct populations of cylindrical, rodlike nanoparticles, or the presence of particles of any one or more alternative (nonspherical) morphologies.

When the Au nanoparticles are freed from the ionogel matrix and suspended in ethanol, a pale-pink solution is obtained whose UV/Vis–NIR spectrum (Figure 3B) retains the general features of the spectrum of the gold–ionogel composite (in particular, a broad band at ca. 585 nm that extends significantly into the NIR region), but lacks discernible bands in the mid-wavelength and NIR regions. This change may be explained by either morphological alterations induced in the particles by their release from the ionogel or disruption of nanoparticle organization or aggregation.[51] Notably, the ease with which the nanoparticles can be isolated (i.e., by simply dissolving the ionogel matrix in a small volume of ethanol) provides an excellent illustration of one of the principal advantages of in situ synthesis of nanoparticles within soft materials.

Our conclusions regarding the shape of the Au nanoparticles derived from the UV/Vis–NIR spectroscopy, namely, that the nanoparticles are primarily nonspherical and comprise a mixture of morphologies, are supported by the results of characterization studies of the particles embedded in a thin film of the ionogel using high-resolution scanning electron microscopy (SEM). The measurements were taken from the sample employed for the SAXS studies described above by fracturing the capillary containing it and transferring the sample onto an SEM holder. The results of direct microstructural examination of the particles are presented in Figure 4. (It is important to note in these micrographs that although some of the gold nanoparticles protrude from the gel matrix, the majority are embedded in it and thus are subsurface. As a consequence, most of the particles will appear to be slightly out of focus, a result of multiple scattering effects.) As can be seen from Figure 4A, nanoparticles of a variety of sizes (ranging from ca. 100 to 1000 nm) and morphologies are present, and include particles with hexagonal, trapezoidal, and rectangular shapes. Most notable is the presence of a number of triangular and icosahedral particles, close-up images of which are shown in Figure 4B and D, respectively. Many of the triangular particles possess sharp vertices, but their corners are often truncated to varying degrees. Notably absent are large numbers of the spherical nanoparticles typically observed upon reduction of tetrachloroaurate in isotropic media. Energy-dispersive X-ray (EDX) spectroscopy (Figure 4F) carried out on isolated particles demonstrates that the major component is gold; the additional elemental species present (C, Si, Cl) are attributable to either the supporting ionogel matrix or the sample support.

The assortment of morphologies observed here resembles that obtained upon ultrasonic irradiation of an ethylene glycol solution of hydrogen tetrachloroaurate in the presence of a capping reagent.[55] However, another SEM image collected on the same Au–ionogel nanocomposite (Figure 4C) reveals what may represent a significant distinction between the particles generated in the ionogel and those re-
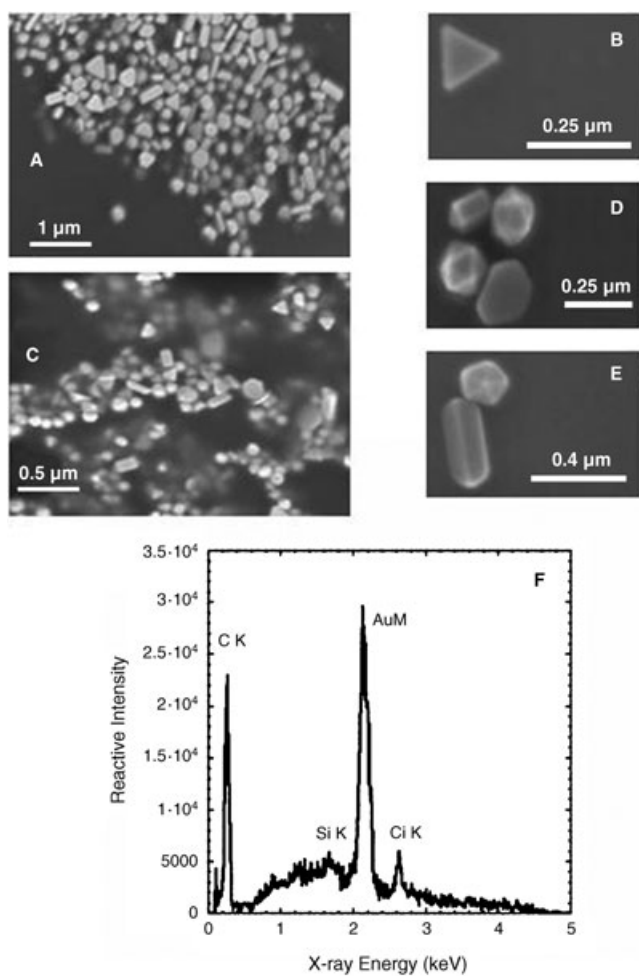
Figure 4. SEM images collected on a glass-supported $C_{10}mim^+Cl^-$ sample containing about 16% (w/w) 0.02 M aqueous $HAuCl_4$ after UV irradiation for 70 min (photoirradiation was carried out in a glass capillary). A) Region showing a large collection of nanoparticles adopting a variety of morphologies. B) Image of an isolated triangular nanoparticle. C) Image indicating the presence of trigonal prismatic nanorods. D) High-resolution image of a trigonal prismatic nanorod. E) High-resolution image of a second type of prismatic nanorod. F) EDX spectrum of a representative trigonal prismatic nanorod.

ported previously. That is, prior reports of triangular metal nanoparticles have described platelets whose thickness corresponds to only a small fraction of the edge length of the triangle. Jin et al.,[56] for example, reported photoinduced morphological changes in silver nanospheres that yielded triangular particles whose thickness (15.6 ± 1.4 nm) constituted only about 20% of the edge length. Similarly, Li et al.[55] reported the formation of triangular gold platelets (of unspecified dimensions) among the variety of morphologies generated upon ultrasonic irradiation of various tetrachloroauric acid solutions. In contrast, Figure 4C and D (upper left image) clearly shows that not all of the triangular nanoparticles formed within the ionogel are thin plates, as in several instances the particle thickness exceeds the edge length by at least a factor of two. Given that the definition of the term "nanorod" encompasses nanoparticles having a width of ≈ 1–100 nm and an aspect ratio greater

than 1 but less than 20,[57] we regard "trigonal prismatic nanorod" as the most appropriate description of these particles. Small amounts of a second type of prismatic nanorod, one whose ends appear to comprise pentagonal pyramids, are also present (Figure 4E). Regardless of their morphology, the nanoparticles imaged by SEM are clearly larger than the water channels of the ionogel, and thus have been displaced from the matrix and reside "above" rather than within the ionogel. The formation of particles whose sizes exceed the dimensions of the template is not uncommon for soft condensed-matter phases, and has been observed for micellar templates.[58]

To further characterize the morphology of the gold nanoparticles, TEM measurements were carried out on particles liberated from the ionogel by dissolution of the glass-supported film in methanol following deposition of the resuspended particles on holey-carbon-on-copper grids. A low-resolution, bright-field image (100 kV) of a representative collection of nanoparticles clearly shows the same assortment of particle morphologies present in the SEM images, which includes triangular and hexagonal particles (data not shown). Energy-dispersive X-ray spectroscopy carried out on the nanoparticles also yielded a spectrum showing gold as the major component, with the remaining peaks arising from the supporting copper TEM grid.

3. Conclusions

Taken together, the results of the UV/Vis–NIR and electron microscopy studies demonstrate that photochemical reduction of $AuCl_4^-$ in an ionogel matrix results in the formation of a mixture of asymmetric gold nanoparticles comprising a variety of sizes and morphologies, among them triangular plates and prismatic rods. The highly constrained water channels within the lyotropic liquid-crystalline ionogel phase clearly play an important role in the process leading to nanoparticle formation, although the exact templating mechanism remains unclear. Also unclear are the details of the association between the ionic liquid and the nucleating gold nanoparticles in this system. Whatever the exact nature of this interaction, it appears likely that $C_{10}mim^+Cl^-$ does play a role in the stabilization of the nanoparticles. (It has been hypothesized that the stabilization of the unstable (100) surface of cylindrical gold nanorods synthesized within cationic micelles such as hexadecyltrimethylammonium bromide may be the result of halide binding and charge transfer to the gold atoms on the (100) surface.[59] A similar mechanism may be operative here.) The $C_{10}mim^+$ cation may serve initially to trap or localize the $AuCl_4^-$ through electrostatic interactions, then after particle formation, to provide a protective sheath around the particles, thus stabilizing them. Clearly too, the structure of the self-assembled $C_{10}mim^+Cl^-$ ionogel must direct the morphology of the nanoparticles that nucleate and grow within it. Finally, as we have noted, in the presence of gold nanoparticles the ionogel can adopt a near-monodomain structure. Such synergistic interactions, in which the formation of a guest component promotes a more ordered host structure, while a

hallmark of nature (in biomineralization, for example), are only rarely achieved synthetically.[60] With further refinement of the photochemical synthesis of the nanoparticles, it may be possible to prepare ordered composites containing arrays of gold nanoparticles embedded in a highly ordered hydrogel matrix, thus permitting precise control over interparticle spacing. Such nanocomposite materials may be useful in a variety of applications, such as plasmonics, in which control of both particle morphology and spacing is critical in determining function.

The details of the interplay between the matrix and the nucleation and stabilization of inorganic nanoparticles within it remain to be determined, but our results raise the possibility of achieving control of particle morphology by careful selection of the ionogel template. Indeed, as we have recently demonstrated,[33] merely adjusting the water content of the ionogel can lead to dramatic changes in its mesoscopic structure, changes which ultimately may be exploited to permit the facile selection and tuning of the optical, electronic, and catalytic properties of nanoparticles. This work underscores the potential of soft materials such as hydrogels in the development of comprehensive, predictable schemes for both the synthesis of nanoscale building blocks and their assembly into highly integrated, functional composite materials.

4. Experimental Section

Sample preparation: The ionic liquid (IL) 1-decyl-3-methylimidazolium chloride ($C_{10}mim^+Cl^-$) was prepared as previously described.[29] After drying in vacuo at 70°C for 48 h, the IL was characterized by ^1H and ^{13}C NMR spectroscopy and by high-resolution fast atom bombardment mass spectrometry (FAB-MS; Washington University Mass Spectrometry Resource, St. Louis, MO). The water content of the IL was determined by Karl Fischer titration (ANL Analytical Services Department). The IL gel was formed by addition of a $HAuCl_4$ solution (0.02 M) to $C_{10}mim^+Cl^-$ to yield a mixture with a total water content of 16–17% (w/w). A uniform gel phase was obtained by repeated gentle heating and vortex mixing. The gel was then irradiated with 254-nm UV light (450 W, 7830 ACE-Havovia) for 30–70 min. Nanopure water was used in the preparation of all aqueous solutions.

Physical methods: UV/Vis–NIR absorption spectra were recorded either on a Cary model 5G UV/Vis–NIR spectrophotometer or an Ocean Optics (Dunedin, FL) SD2000 fiber-optic spectrometer. Small-angle X-ray scattering (SAXS) measurements were made using the instrument at undulator beamline 12ID-C of the Advanced Photon Source at Argonne National Laboratory. The sample-to-detector distance was such as to provide a detecting range for momentum transfer of $0.0025 < q < 0.6$ Å^{-1}. The scattering vector q was calibrated using silver behenate standard at $q = 1.076$ Å^{-1}. The 2D scattering images were first corrected for the spatial distortion and sensitivity of the detector, then radially averaged to produce plots of scattered intensity $I(q)$ versus scattering vector q, the value of which is proportional to the inverse

of the length scale, Å^{-1}. Samples were sealed in 1.5-mm quartz or glass capillaries.

SEM was conducted on a Hitachi S4700 field-emission-gun scanning electron microscope operated between 1.5 and 5 kV. Samples were prepared by fracturing the capillary tube containing the ionogel/nanoparticle mixture and either directly imaging the contents of the tube or transferring a small quantity of the mixture onto a standard SEM holder.

Transmission electron microscopy (TEM) was performed on a Philips model CM30 instrument equipped with an EDX spectrometer operated at an accelerating voltage of 100 kV. Samples were prepared by dissolving the ionogel in methanol, adding the solution dropwise to a holey carbon grid, and evaporating the methanol.

[1] E. Katz, A. Shipway, I. Willner in *Nanoscale Materials* (Eds.: L. M. Liz-Marzan, P. V. Kamat), Kluwer, London, **2003**, pp. 5–64.
[2] R. M. Crooks, V. Chechik, *J. Am. Chem. Soc.* **2000**, *122*, 1243–1244.
[3] Y. Dirix, C. Bastiaansen, W. Caseri, P. Smith, *Adv. Mater.* **1999**, *11*, 223–227.
[4] W. L. Barnes, A. Dereux, T. W. Ebbesen, *Nature* **2003**, *424*, 824–830.
[5] S. A. Maier, P. G. Kik, H. A. Atwater, S. Meltzer, E. Harel, B. E. Koel, A. A. G. Requicha, *Nat. Mater.* **2003**, *2*, 229–232.
[6] A. J. Haes, R. P. Van Duyne, *J. Am. Chem. Soc.* **2002**, *124*, 10596–10604.
[7] Y. W. C. Cao, R. C. Jin, C. A. Mirkin, *Science* **2002**, *297*, 1536–1540.
[8] T. R. Jensen, M. L. Duval, K. L. Kelly, A. A. Lazarides, G. C. Schatz, R. P. Van Duyne, *J. Phys. Chem. B* **1999**, *103*, 9846–9853.
[9] C. L. Haynes, A. D. McFarland, L. L. Zhao, R. P. Van Duyne, G. C. Schatz, L. Gunnarsson, J. Prikulis, B. Kasemo, M. Kall, *J. Phys. Chem. B* **2003**, *107*, 7337–7342.
[10] M. B. Mohamed, V. Volkov, S. Link, M. A. El-Sayed, *Chem. Phys. Lett.* **2000**, *317*, 517–523.
[11] G. Schider, J. R. Krenn, W. Gotschy, B. Lamprecht, H. Ditlbacher, A. Leitner, F. R. Aussenegg, *J. Appl. Phys.* **2001**, *90*, 3825–3830.
[12] M. Valden, X. Lai, D. W. Goodman, *Science* **1998**, *281*, 1647–1650.
[13] D. I. Gittins, D. Bethell, D. J. Schiffrin, R. J. Nichols, *Nature* **2000**, *408*, 67–69.
[14] D. Appell, *Nature* **2002**, *419*, 553–555.
[15] C. R. Martin, *Chem. Mater.* **1996**, *8*, 1739–1746.
[16] B. M. I. van der Zande, M. R. Bohmer, L. G. J. Fokkink, C. Schonenberger, *Langmuir* **2000**, *16*, 451–458.

[17] C. Schonenberger, B. M. I. van der Zande, L. G. J. Fokkink, M. Henny, C. Schmid, M. Kruger, A. Bachtold, R. Huber, H. Birk, U. Staufer, *J. Phys. Chem. B* **1997**, *101*, 5497–5499.

[18] C. R. Martin, M. Nishizawa, K. Jirage, M. Kang, *J. Phys. Chem. B* 2**0**01, 105, 1925–1934.

[19] T. A. Crowley, K. J. Ziegler, D. M. Lyons, D. Erts, H. Olin, M. A. Morris, J. D. Holmes, *Chem. Mater.* **2003**, *15*, 3518–3522.

[20] M. Mandal, S. K. Ghosh, S. Kundu, K. Esumi, T. Pal, *Langmuir* **2002**, *18*, 7792–7797.

[21] L. M. Huang, H. T. Wang, Z. B. Wang, A. P. Mitra, D. Zhao, Y. H. Yan, *Chem. Mater.* **2002**, *14*, 876–880.

[22] C. Faure, A. Derre, W. Neri, *J. Phys. Chem. B* **2003**, *107*, 4738–4746.

[23] J. X. Gao, C. M. Bender, C. J. Murphy, *Langmuir* **2003**, *19*, 9065–9070.

[24] M. A. Firestone, D. M. Tiede, S. Seifert, *J. Phys. Chem. B* **2000**, *104*, 2433–2438.

[25] M. Andersson, V. Alfredsson, P. Kjellin, A. E. C. Palmqvist, *Nano Lett.* **2002**, *2*, 1403–1407.

[26] J. D. Holbrey, K. R. Seddon, *Clean Products Processes* **1999**, *1*, 223–236.

[27] M. J. Earle, K. R. Seddon, *Pure Appl. Chem.* **2000**, *72*, 1391–1398.

[28] P. Wasserscheid, T. Welton, *Ionic Liquids in Synthesis*, Wiley-VCH, Weinheim, **2003**.

[29] M. A. Firestone, J. A. Dzielawa, P. Zapol, L. A. Curtiss, S. Seifert, M. L. Dietz, *Langmuir* **2002**, *18*, 7258–7260.

[30] M. L. Dietz, J. A. Dzielawa, M. P. Jensen, M. A. Firestone in *Ionic Liquids as Green Solvents: Progress and Prospects*, Vol. 856 (Eds.: R. D. Rogers, K. R. Seddon), American Chemical Society, Washington, DC, **2003**, pp. 526–543.

[31] Y. Zhou, J. H. Schattaka, M. Antoniette, *Nano Lett.* **2004**, *4*, 477–481.

[32] N. Kimizuka, T. Nakashima, *Langmuir* **2001**, *17*, 6759–6761.

[33] M. A. Firestone, P. G. Rickert, S. Seifert, M. L. Dietz, *Inorg. Chim. Acta* **2004**, *357*, 3991–3998.

[34] J. Dupont, G. S. Fonseca, A. P. Umpierre, P. F. P. Fichtner, S. R. Teixeira, *J. Am. Chem. Soc.* **2002**, *124*, 4228–4229.

[35] J. Huang, T. Jiang, B. Han, H. Gao, Y. Chang, G. Zhao, W. Wu, *Chem. Commun.* **2003**, 1654–1655.

[36] G. S. Fonseca, A. P. Umpierre, P. F. P. Fichtner, S. R. Teixeira, J. Dupont, *Chem. Eur. J.* **2003**, *9*, 3263–3269.

[37] C. W. Scheeren, G. Machado, J. Dupont, P. F. P. Fichtner, S. R. Tex-eira, *Inorg. Chem.* **2003**, *42*, 4738–4742.

[38] K. Anderson, S. C. Fernandez, C. Hardacre, P. C. Marr, *Inorg. Chem. Commun.* **2004**, *7*, 73–76.

[39] Y. J. Zhu, W. W. Wang, R. J. Qi, X. L. Hu, *Angew. Chem.* **2004**, *116*, 1434–1438; *Angew. Chem. Int. Ed.* **2004**, *43*, 1410–1414.

[40] J. Dupont, *J. Braz. Chem. Soc.* **2004**, *15*, 341–350.

[41] I. Pastoriza-Santos, L. M. Liz-Marzan, *Langmuir* **2002**, *18*, 2888–2897.

[42] N. A. Melosh, P. Davidson, B. F. Chmelka, *J. Am. Chem. Soc.* **2000**, *122*, 823–829.

[43] I. W. Hamley, M. D. Gehlsen, A. K. Khandpur, K. A. Koppi, J. H. Rosedale, M. F. Schulz, F. S. Bates, K. Almdal, K. Mortensen, *J. Phys. II Fr.* **1994**, *4*, 2161–2186.

[44] C. Y. Wang, T. P. Lodge, *Macromolecules* **2002**, *35*, 6997–7006.

[45] L. M. Bronstein, D. I. Svergun, A. R. Khokhlov, *Polymer Gels and Networks*, Marcel Dekker, New York, **2002**, pp. 103–130.

[46] M. D. Malinsky, K. L. Kelly, G. C. Schatz, R. P. Van Duyne, *J. Phys. Chem. B* **2001**, *105*, 2343–2350.

[47] Y. G. Sun, Y. N. Xia, *Analyst* **2003**, *128*, 686–691.

[48] T. J. Norman, C. D. Grant, D. Magana, J. Z. Zhang, J. Liu, D. L. Cao, F. Bridges, A. Van Buuren, *J. Phys. Chem. B* **2002**, *106*, 7005–7012.

[49] Y. Y. Yu, S. S. Chang, C. L. Lee, C. R. C. Wang, *J. Phys. Chem. B* **1997**, *101*, 6661–6664.

[50] T. K. Sau, C. J. Murphy, *J. Am. Chem. Soc.* **2004**, *126*, 8648–8649.

[51] N. Malikova, I. Pastoriza-Santos, M. Schierhorn, N. A. Kotov, L. M. Liz-Marzan, *Langmuir* **2002**, *18*, 3694–3697.

[52] O. P. Varnavski, M. B. Mohamed, M. A. El-Sayed, T. Goodson, *J. Phys. Chem. B* **2003**, *107*, 3101–3104.

[53] F. Kim, J. H. Song, P. D. Yang, *J. Am. Chem. Soc.* **2002**, *124*, 14316–14317.

[54] F. Kim, S. Connor, H. Song, T. Kuykendall, P. D. Yang, *Angew. Chem.* **2004**, *116*, 3759–3763; *Angew. Chem. Int. Ed.* **2004**, *43*, 3673–3677.

[55] C. Li, W. Cai, C. Kan, G. Fu, L. Zhang, *Mater. Lett.* **2003**, *58*, 196–199.

[56] R. C. Jin, Y. W. Cao, C. A. Mirkin, K. L. Kelly, G. C. Schatz, J. G. Zheng, *Science* **2001**, *294*, 1901–1903.

[57] C. J. Murphy, N. R. Jana, *Adv. Mater.* **2002**, *14*, 80–82.

[58] M. P. Pileni, *Nat. Mater.* **2003**, *2*, 145–150.

[59] Z. L. Wang, R. P. Gao, B. Nikoobakht, M. A. El-Sayed, *J. Phys. Chem. B* **2000**, *104*, 5417–5420.

[60] S. Weiner, L. Addadi, *J. Mater. Chem.* **1997**, *7*, 689–702.